BEAM TRANSPORT EXPERIMENTS OVER HALF-TURN AT THE UNIVERSITY OF MARYLAND ELECTRON RING (UMER)*

S. Bernal†, B. Beaudoin, Y. Cui, D. Feldman, R. Feldman, M. Glanzer, T. Godlove, I. Haber, J. Harris, M. Holloway, Y. Huo, R.A. Kishek, D. Lamb, W-T. Lee, H. Li, B. Quinn, M. Reiser, A. Valfells, M. Walter, M. Wilson, R. Yun, Y. Zou, and P.G. O'Shea,
Institute for Research in Electronics and Applied Physics,
University of Maryland, College Park, MD 20742

Abstract

The University of Maryland Electron Ring (UMER), designed for studies of space-charge dominated beam transport in a strong focusing lattice, is nearing completion. UMER models, for example, the recirculator machine envisioned as a possible driver for heavy-ion inertial fusion. The UMER lattice consists of 36 FODO periods distributed among 18, 20^0-bending sections containing two dipole magnets each. The main diagnostics are phosphor screens and capacitive beam position monitors placed at the center of each bending section. In addition, pepper-pot and slit-wire emittance meters, as well as an energy analyzer are in operation. We present here results of beam matching and characterization for a range of currents extending from about 1 mA to 100 mA, all at 10 keV and 100 ns pulse duration. With typical focusing given by σ_0=76^0, the zero-current betatron phase advance per period, the range of currents corresponds to tune depressions of 0.8 to 0.2. This range covers both the emittance dominated and extreme space-charge dominated regimes, which is unprecedented for a circular machine.

INTRODUCTION

The University of Maryland Electron Ring (UMER) is designed for *scaled* experiments employing low energy (up to 10 keV), high current (up to 100 mA) electron beams. A general description and motivation of the ring can be found in the UMER web page [1] and recent publications [2]. The development of individual components has been presented in papers at the 1999 and 2001 PACs, and updates appear in these Proceedings. Construction of a machine with a layout similar to UMER's was undertaken a few years ago at Lawrence Livermore National Laboratory. In the Livermore ring, a 80 keV (initial energy) potassium-ion beam was successfully transported and accelerated over one quarter turn [3]. In this paper, we report on results of electron beam transport experiments over one-half turn, i.e. 18 FODO periods. A detailed account of experiments over one-quarter turn was submitted for publication [4].

* Work supported by the U.S. Department of Energy.
† sabern@glue.umd.edu

LAYOUT AND DIAGNOSTICS

A photograph of the current UMER setup and the corresponding schematics are shown in Figure 1. The DC injector consists of a short solenoid, seven printed-circuit (PC) quadrupoles, a DC bending dipole, a number of elements for beam steering, and two sets of Helmholtz coils for balancing of the Earth's magnetic field. Results of rms envelope matching experiments with a former version of the injector were presented before [5]. The former DC injector employed six PC quadrupoles instead of seven, over a distance of one meter, approximately. The new DC injector not only provides a smoother transition into the periodic FODO lattice, but also fits the geometry of the pulsed, Y-shaped injector which is nearing completion (see M. Walter et al, TPPB025 paper in these proceedings.)

Nine bending sections (labeled RC1 through RC9 in Fig. 1) follow the matching/injection section. Each section contains two FODO periods, i.e. four PC quadrupoles and two PC bending dipoles, and a diagnostics chamber between the quadrupoles in the straight part. In addition, short PC steering dipoles for vertical steering are placed over the 4-1/2" flanges between sections. An important feature of UMER is that it takes advantage of the bending action of the Earth's magnetic field on the 10 keV electron beam. Thus, the required current on the PC bending dipoles is reduced from near 3.0 A to about 2.5 A.

The diagnostics in the straight section include a phosphor screen (chamber labeled IC1 in Fig. 1), a combination beam-position monitor (BPM)- Phosphor Screen (at IC2), and a fast Bergoz transformer between quadrupoles Q2 and Q3 for current measurements. The chambers in the ring sections also have a combination BPM-Phosphor Screen. The beam image is reflected at a mirror oriented at 45^0 and monitored through a window in each diagnostics chamber (Fig. 1). The phosphor screen/mirror housing is attached to the bottom plate of the BPM, so either one can be placed in line by means of an actuator. The BPMs are multiplexed and computer monitored (see B. Quinn et al, WPPB073 paper in these proceedings.) . End diagnostics include a second Bergoz coil near the entrance to the large diagnostics chamber and a magnetically-actuated phosphor screen system. The large diagnostic chamber houses a pepper-pot for integrated emittance measurements, as well as a slit-wire assembly for both horizontal and vertical, time-resolved

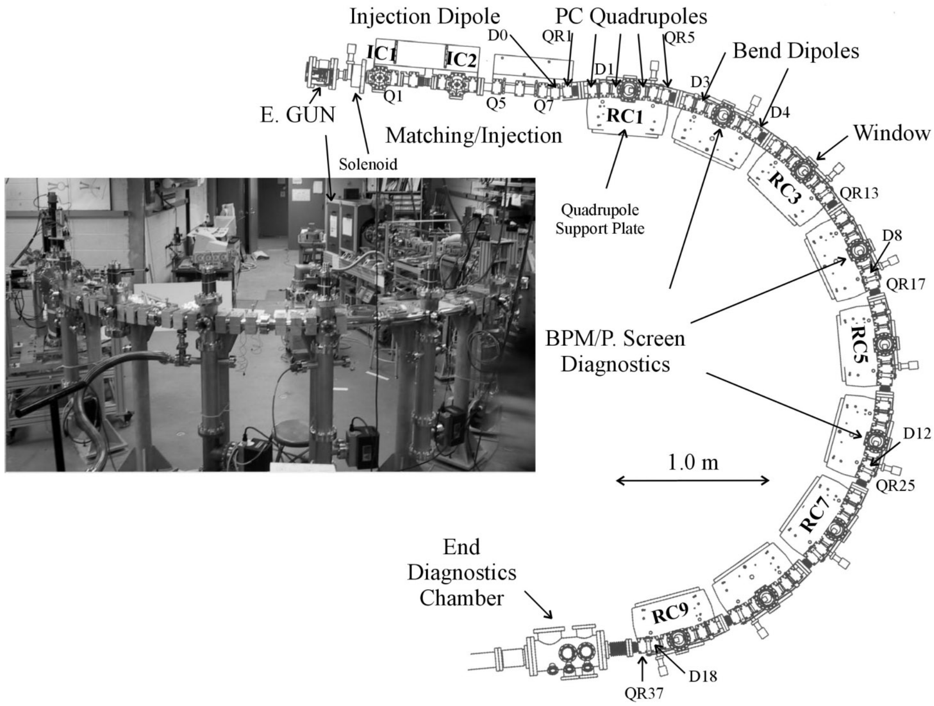

Figure 1: Photo and schematics of current UMER experiment. See text for explanation on labels.

emittance measurements (see M. Walter et al, TPPB074 paper in these proceedings.)

Lastly, we have installed a Nd:YAG laser near the exit of the UMER electron gun and demonstrated photoemission from the dispenser cathode. With pulse energies of 1-2 mJ in the 2nd and 3rd harmonics, we are able to obtain space-charge limited current pulses (100 mA) with pulse widths of 4.5ns. By adjusting the cathode temperature, we can produce combined thermionic and photoelectric pulses, and with suitable masks in the optical path, we have produced multiple beamlets from the UMER cathode. The new photoinjector has already proved to be a useful tool for initial studies of longitudinal beam dynamics (see A. Valfells et al, WPAG020 paper in these proceedings.)

Table 1: Beam Parameters (10keV, σ_0=76^0, ϵ=4×rms, unnormalized emittance)

Current (mA)	Initial ϵ (μm)	Avg. Beam Radius (mm)	Tune Depression
0.55±5%	5±20%	1.3	0.8
24±2%	30	5.3	0.3
85±2%	55	9.5	0.16

BEAM ALIGNMENT AND RMS ENVELOPE MATCHING

Experiments were conducted with three different beam currents (see Table 1), the lowest one corresponding to an emittance-dominated beam and the other two in the region of extreme space-charge dominated transport. No current losses were measured for the 0.55 and 24 mA beams, but a <5% loss may occur for the 85 mA beam, which is attributable to halo particles from envelope mismatch. Beam-based alignment, on the other hand, varies from the lowest current cases to the 85 mA case, i.e. the steering dipoles have to be set differently for the highest current. This can be understood by the fact that beam- centroid drift from image forces, in addition to beam distortions from quadrupole rotation errors, plays a larger role for the highest current.

Beam-based alignment was done with the BPMs as follows: the "Left−Right" and "Top−Bottom" electrode signals from a BPM were minimized for different bending currents in the two bending dipoles upstream of the BPM chamber. The correct bending-currents pair was obtained by a scan of the quadrupole upstream of the BPM. As an example, the currents of dipoles D2 and D3 (Fig. 1) are varied and the BPM on RC1 monitored. The correct pair of currents, i.e. the one that gives both correct centroid and beam angle through the BPM, is chosen after current scans (±1.0 A) of QR3. The error in centroid location from this procedure is ±0.1 to ±0.4 mm, depending on beam current (see B. Quinn et al, WPPB073 paper in these proceedings.)

As mentioned above, another important factor in the experiments is the error in quadrupole rotation about the magnetic axis. Although the four quadrupoles in a given 20^0 bending section share a common support plate (see Fig. 1), there are small differences in roll angle among

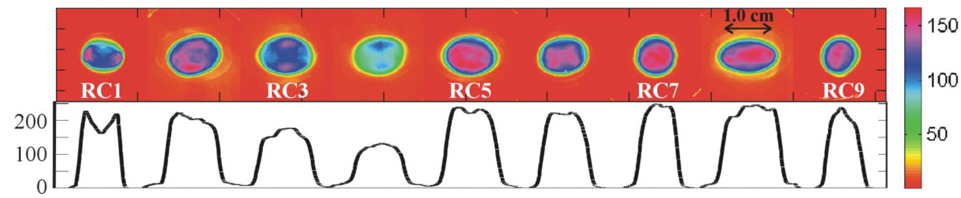

Figure 2: False-color rendering of fluorescent screen pictures of 24 mA beam (see Table 1) in the nine ring chambers, and horizontal straight-cut density profiles (8-bit grayscale, unnormalized).

the quadrupoles arising from assembly, mounting and other mechanical factors. Furthermore, the support plates in all ring chambers do not share exactly the same plane, despite an effort to adjust them with the help of an optical alignment system (see M. Walter et al, WPPB075 paper in these proceedings.) In order to alleviate the problem, the quadrupole mounts were individually leveled with an error of $\pm$1.0 mrad. Still, a residual effect of these errors is obvious in the beam cross section orientation, as seen in the picture montage of Figure 2 for the 24 mA beam. We should add that the CCD camera itself was leveled with the same accuracy as for the quadrupole mounts.

Initial rms envelope-matching calculations for the 24 mA beam (at 10 keV) are based on a straight FODO lattice (see [5]). The effective (2 rms) experimental beam radii in the two transverse directions are obtained from the fluorescent screen pictures. As can be seen in the picture montage of Fig. 2, the vertical dimension of the beam is essentially constant if one excludes the visible halo. However, the horizontal dimension shows a sudden increase, accompanied by an extended halo, from RC7 to RC8. Pepperpot emittance measurements, on the other hand, yield $\epsilon_{x,y}$=42,28 $\pm 5\mu$m at the end of the 180^0 system, compared with $\epsilon_{x,y}$=30,36 $\pm 5\mu$m from previous experiments over four ring chambers (i.e. a 90^0 bend). The value of initial emittance quoted in Table 1 is the number expected from linearly scaling the measured initial emittance of the full 100 $\pm$ 5mA beam. This scaling is based on the use of a 1.5 mm (radius) aperture to obtain the 24 mA beam. Finally, time-integrated measurements with the slit-wire system yield $\epsilon_{x,y}$=30,20μm, but a comparison between results from the two emittance meters is not straightforward.

The experiment with the 85 mA beam yields pictures with features similar to those of the 24 mA beam, except for generally larger cross section tilts. The first pepperpot emittance measurements, on the other hand, reveal an increase of 20-25% over the 90^0-system results, but additional tests that include the slit-wire meter are needed.

Other features under investigation are the possibility of transverse waves in the beam (see bottom of Fig. 2), associated anisotropy, dispersive and bunch-end effects, energy spread evolution and other studies of longitudinal dynamics. Concerning the latter, an accompanying paper presents results on the evolution of non-square current profiles in the ring (see A. Valfells et al, WPAG020 paper in these proceedings.)

CONCLUSION

We have demonstrated emittance as well as space-charge dominated beam transport in a 180^0 bend system. We are developing the "single-turn" beam physics in UMER as we build the machine. Foremost are beam-based alignment and envelope matching. They are increasingly more difficult for higher currents, despite better S/N in the signals from the capacitive BPMs. This is so because of the role of image forces and quadrupole rotation errors. The way bending couples with these effects is still under study, and its understanding should provide the means for transport with minimum emittance growth, a prerequisite for multi-turn operation in UMER.

REFERENCES

[1] http://www.ipr.umd.edu/ebte/ring/

[2] P.G. O'Shea et al., "Experiments with Space-Charge-Dominated Beams for Heavy-ion Fusion Applications", Laser and particle beams, 20, 599-602 (2002). P.G. O'Shea et al, Nucl. Instr. Phys. Res. A **464**, 646-652 (2001).

[3] L. Ahle et al., "Results from the Recirculator Project at LLNL", Nucl. Instr. Phys. Res. A **464**, 557-562 (2001).

[4] S. Bernal et al., submitted to Nucl. Instr. Phys. Res. A.

[5] S. Bernal et al., "Beam Tests of the 10 keV Injector for the University of Maryland Electron Ring (UMER)", Proc. PAC 2001, Chicago, Ill (2001).